HAL
open science

Channel Impulsive Noise Mitigation for Linear Video Coding Schemes

S Zheng, M. Cagnazzo, Michel Kieffer

To cite this version:

S Zheng, M. Cagnazzo, Michel Kieffer. Channel Impulsive Noise Mitigation for Linear Video Coding Schemes. ICASSP 2019 - 2019 IEEE International Conference on Acoustics, Speech and Signal Processing (ICASSP), May 2019, Brighton, United Kingdom. 10.1109/icassp.2019.8682699 . hal-02109233

HAL Id: hal-02109233

https://telecom-paris.hal.science/hal-02109233v1

Submitted on 24 Apr 2019

HAL is a multi-disciplinary open access archive for the deposit and dissemination of scientific research documents, whether they are published or not. The documents may come from teaching and research institutions in France or abroad, or from public or private research centers.

L'archive ouverte pluridisciplinaire **HAL**, est destinée au dépôt et à la diffusion de documents scientifiques de niveau recherche, publiés ou non, émanant des établissements d'enseignement et de recherche français ou étrangers, des laboratoires publics ou privés.

CHANNEL IMPULSIVE NOISE MITIGATION FOR LINEAR VIDEO CODING SCHEMES

S. Zheng, M. Cagnazzo

LTCI, Télécom ParisTech,
Univ Paris-Saclay,75013, Paris, France.

M. Kieffer

L2S, CNRS–CentraleSupelec–Univ Paris-Sud,
Univ Paris-Saclay, 3 rue Joliot-Curie,
91192 Gif-sur-Yvette, France.

ABSTRACT

This paper considers the problem of impulse noise mitigation when video is encoded using a SoftCast-based Linear Video Coding (LVC) scheme and transmitted using an Orthogonal Frequency-Division Multiplexing (OFDM) scheme over a wideband channel prone to impulse noise. In the time domain, the impulse noise is modeled as independent and identically distributed (iid) Bernoulli-Gaussian variables. A Fast Bayesian Matching Pursuit algorithm is employed for impulse noise mitigation. This approach requires the provisioning of some OFDM subchannels to estimate the impulse noise locations and amplitudes. Provisioned subchannels cannot be used to transmit data and lead to a decrease of the video quality at receivers in absence of impulse noise. Using a phenomenological model (PM) of the residual noise variance after impulse mitigation, we have proposed an algorithms that is able to evaluate the optimal number of subchannels to provision for impulse noise correction. Simulation results show that the PM can accurately predict the number of subchannels to provision and that impulse noise mitigation can significantly improve the decoded video quality compared to a situation where all subchannels are used for data transmission.

***Index Terms*—** Video transmission. SoftCast. OFDM. Impulse noise correction. Sparse vector estimation. Optimization.

1. INTRODUCTION AND MAIN CONTRIBUTIONS

SoftCast [9] based Linear video coding (LVC) and transmission schemes [2, 4–8, 10, 13–15, 18, 22–27] have emerged as a promising alternative to classical video coding [19–21] when video has to be transmitted to wireless receivers experiencing different and time-varying channel conditions. In LVC, the video content is encoded with linear-only operators, such as a full-frame Discrete Cosine Transform (DCT) and using linear channel precoding of these DCT coefficients. Since the transmitted symbols are linearly related to the original video pixel values and a Linear Minimum Mean Square Error (LMMSE) estimator is used at receiver side, the decoded video quality scales linearly with the channel signal-noise-ratio (SNR) [9].

In this paper, we address the problem of impulse noise mitigation when the LVC-encoded video is transmitted using an Orthogonal Frequency-Division Multiplexing (OFDM) scheme over a wideband channel prone to impulse noise. Many communication channels may be also prone to impulse noise, *e.g.*, in Power Line Telecommunications (PLT) channels [29]. Impulse noise has a high magnitude (its power may be 50dB above that of the background noise), and when it is bursty, may corrupt the channel for more than 1 ms. If impulse noise is not corrected, the communication performance may be significantly degraded [1, 12]. As in [1], the impulse noise is modeled in the time domain by iid Bernoulli-Gaussian variables. In here Fast Bayesian Matching Pursuit (FBMP) [17] algorithm is employed for impulse noise mitigation. This approach requires the provisioning of some OFDM subchannels to estimate the impulse noise locations and amplitudes. Since nothing can be transmitted on provisioned subchannels, this leads to a decrease of the number of transmitted chunks and to a decrease of the video quality at receivers in absence of impulse noise. A trade-off has thus to be found between impulse noise correction efficiency and nominal PSNR reduction.

Compared to the state-of-the-art, our contributions are (*i*) adapt FBMP in channel impulse noise mitigation for LVC schemes; (*ii*) propose a phenomenological model (PM) structure to describe the variance of residual noise after impulse noise mitigation. (*iii*) By using this PM to provide an algorithm for the selection of the optimal number of subchannels to provision for impulse noise correction. Simulation results illustrate the performance improvements provided by the proposed impulse noise mitigation scheme.

The rest of the paper is organized as follows. The application of FBMP for impulse noise mitigation to LVC scheme is described in Section 2. Section 3 presents the way the optimal number of subchannels to provision can be determined for impulse noise correction. Simulation results are described in Section 4 before drawing some conclusions in Section 5.

2. IMPULSE NOISE CORRECTION SCHEME FOR LVC

In this section we present the architecture of the proposed impulse noise correction scheme for SoftCast-based [9] LVC architectures, which is shown in Fig. 1. In this paper we focus on Scaling, Impulse Noise Estimation (*INE*), Impulse Noise Mitigation (*INM*) and decoding (LMMSE) modules, while the other steps are the same as in [9].

The input video is organized in Group of Pictures (GoP); each GoP undergoes 3D-DCT and the resulting coefficients are organized in blocks called chunks. The number of chunks per GoP is referred to as n_{Ck}. The chunks are scaled and used to modulate the carriers of an OFDM-based transmission scheme with n_{SC} subchannels; a total power p_{T} is available for each OFDM symbol. In this paper, we focus on the luminance part of the video. The chrominance components undergo a similar processing.

To perform scaling and transmission, $n_{\mathrm{r}} \times n_{\mathrm{c}}$ *chunk vectors* t_i, $i = 1, \ldots, n_{\mathrm{r}} \times n_{\mathrm{c}}$, each of dimension n_{Ck}, are formed by selecting for each vector one coefficient per chunk. The t_is can be seen as realizations of $n_{\mathrm{r}} \times n_{\mathrm{c}}$ iid Gaussian vectors with covariance matrix $\Lambda = \mathrm{diag}(\lambda_1 \ldots \lambda_{n_{\mathrm{Ck}}})$. Without loss of generality, the chunks, are assumed to be sorted according to decreasing variance

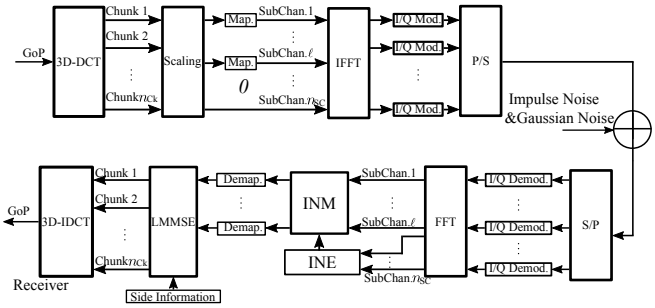

Fig. 1: Proposed architecture for Modified SoftCast-based LVC with subchannel provisioning and impulse noise mitigation. The transmitter and the receiver are shown.

λ_i, $i = 1, \ldots, n_{\rm Ck}$. The chunk vectors are multiplied (scaling) by a diagonal precoding matrix $G \in \mathbb{R}^{n_{\rm SC} \times n_{\rm Ck}}$ [9, 11, 28] designed in such a way that $u_i = Gt_i$ satisfies a power constraint $p_{\rm T}/2$. We focus on a bandwidth constrained scenario where $n_{\rm SC} \leqslant n_{\rm Ck}$. In this case, onlt the first $n_{\rm SC}$ largest variance chunks can be transmitted [9]. Moreover, due to the total power constraint, it is possible that the q lowest-variance chunks must further be discarded [11, 28]. In our proposed architecture, it is possible to discard chunk even when there is enough available transmission power, since this operation will improve the robustness towards impulse noise, as shown later on. In any case, when we discard q chunks, the last q rows of G are null.

Then, $n_{\rm r} \times n_{\rm c}/2$ vectors of complex symbols are formed by combining pairs of consecutive scaled chunk vectors: $\widetilde{u}_i = G\left(t_{2i-1} + jt_{2i}\right)$, $i = 1, \ldots, n_{\rm r} \times n_{\rm c}/2$; the power of $\widetilde{u}_i$ is $p_{\rm T}$. Next the $\widetilde{u}_i$s are used to modulate the OFDM carriers in a standard way. For the sake of simplicity, in what follows the index i is omitted, since all vectors $\widetilde{u}_i$ have similar distribution and undergo the same processing. In the plain Softcast, a Hadamard transform is performed after chunk scaling. Here, to simplify presentation, this additional transform is not considered.

The transmitted signal is assumed to be corrupted by Gaussian noise and impulsive noise. At the receiver side, the input of the FFT is a vector $y \in \mathbb{C}^{n_{\rm SC}}$ that may be modeled as as [1]

$$y \quad = \quad F^H \widetilde{u} + v_{\rm I} + v_{\rm g}, \tag{1}$$

where F^H is IDFT matrix, $v_{\rm g}$ is a Gaussian noise vector and $v_{\rm I}$ is an impulse noise vector. After the DFT, $Fv_{\rm g} \sim \mathcal{CN}\left(0, N_{\rm g}\right)$ can be modeled as a zero-mean complex circular Gaussian noise vector [1] with $N_{\rm g} = 2N$ and $N = \text{diag}\left(\sigma_1^2, \ldots, \sigma_{n_{\rm SC}}^2\right)$, without loss of generality, one assumes that the subchannel indexing is such that $\sigma_1^2 \leqslant \cdots \leqslant \sigma_{n_{\rm SC}}^2$. The components of $v_{\rm I}$ are iid and such that $v_{{\rm I},k} = \delta_k w_k$, where δ_k is the realization of a Bernoulli variable with parameter $p_{\rm I} = \Pr\{\delta_k = 1\}$ and $w_k \sim \mathcal{CN}\left(0, 2\sigma_{\rm I}^2\right)$ with $\sigma_{\rm I}^2 > \sigma_i^2$, $i = 1, \ldots, n_{\rm SC}$.

Since last q rows of G are null, we can introduce the parity-check matrix $\Psi \in \mathbb{C}^{q \times n_{\rm SC}}$ formed by the last q rows of F, and $\Psi F^H G = 0$. Then one may evaluate the *syndrome vector*

$$s = \Psi y = \Psi v_{\rm I} + \Psi v_{\rm g}, \tag{2}$$

where $\Psi v_{\rm g} \sim \mathcal{CN}\left(0, N_s\right)$, with $N_s = 2\text{diag}\left(\sigma_{n_{\rm SC}-q+1}^2, \ldots, \sigma_{n_{\rm SC}}^2\right)$. Therefore to mitigate the effect of the impulse noise, one has to estimate the sparse vector $v_{\rm I}$ from noisy measurements of $\Psi v_{\rm I}$. This is a typical compressive sensing estimation problem [3] for which many solutions have been proposed. Here, FBMP algorithm is employed to get an estimate $\widehat{v}_{\rm I} = \text{E}\left(v_{\rm I}|s\right)$ of $v_{\rm I}$ [17]. This step correspond to *INE* in Figure 1. Finally, after impulse noise mitigation we find $\widehat{y}$:

$$\begin{aligned} \widehat{y} &= Fy - F\widehat{v}_{\rm I} \\ &= \widetilde{u} + F\left(v_{\rm I} - \widehat{v}_{\rm I}\right) + Fv_{\rm g}. \end{aligned} \tag{3}$$

This step correspond to *INM* in Figure 1. In what follows, this scheme is called LVC With Subchannel Provisioning and Impulse Correction (LVC-WSP-IC). The main difficulty lies in the optimization of the number q of subchannels provisioned for impulse noise mitigation. A solution to this problem is detailed in Section 3.

3. OPTIMAL NUMBER OF SUB-CHANNEL PROVISIONING

As shown in [17], the efficiency of the FBMP algorithm increases with the number q of observations of linear combinations of the impulse errors (2). However, increasing q reduces the number of subchannels on which chunk coefficients can be transmitted. A trade-off has thus to be found between efficiency of impulse noise mitigation and transmission performance.

3.1. Residual noise after impulse noise mitigation

One may rewrite (3) as

$$\widehat{y} = \widetilde{u} + Fv_{\rm r} + Fv_{\rm g}, \tag{4}$$

where $v_{\rm r} = v_{\rm I} - \widehat{v}_{\rm I}$ represents the impulse noise residual vector after mitigation. This residual can be seen as an additional noise component to the background Gaussian noise affecting the sub-channels.

As shown in [1] covariance of impulse noise residual $\text{Cov}\left(v_{\rm r}|s\right)$ can be approximated as a diagonal matrix, provided that $n_{\rm SC}$ and q are large enough. Therefore, the covariance matrix of $Fv_{\rm r}|s$ $\text{Cov}\left(Fv_{\rm r}|s\right) = F\text{Cov}\left(v_{\rm r}|s\right)F^H$ has its diagonal elements equal to $\sigma_{\rm r}^2 = \text{Tr}\left(\text{Cov}\left(v_{\rm r}|s\right)\right)/n_{\rm SC}$. Clearly, the off-diagonal entries in $\text{Cov}\left(Fv_{\rm r}|s\right)$ are not zero, but they are neglected in what follows to get

$$\text{Cov}\left(Fv_{\rm r}|s\right) \approx \sigma_{\rm r}^2 I. \tag{5}$$

Considering (4) and (5), the vectors Gt_{2i} and Gt_{2i+1} are corrupted respectively by the real and imaginary parts of $Fv_{\rm r}$ and $Fv_{\rm g}$, with $Fv_{\rm r} \sim \mathcal{CN}\left(0, \sigma_{\rm r}^2 I\right)$. Assuming that $Fv_{\rm r}$ and $Fv_{\rm g}$ are uncorrelated, each component of Gt_{2i} and Gt_{2i+1} will be corrupted by a zero-mean Gaussian noise with variance $\sigma_{{\rm c},i}^2 = \sigma_i^2 + \sigma_{\rm r}^2/2$. By using this in the design of the optimal precoding matrix and decoding matrices, the MSE of the received chunk vector $E\left[\left\|\left(t - \widehat{t}\right)\right\|_2^2\right]$ [11, 28] is

$$\varepsilon = \sum_{i=\ell+1}^{n_{\rm Ck}} \lambda_i + \sqrt{\gamma} \sum_{i=1}^{\ell} \sqrt{\lambda_i \sigma_{{\rm c},i}^2}, \tag{6}$$

where $\ell \leqslant n_{\rm SC}$ is the largest integer such that $\sqrt{\frac{\lambda_i \sigma_{{\rm c},i}^2}{\gamma}} - \sigma_{{\rm c},i}^2 > 0$, $i = 1, \ldots, \ell$ with $\sqrt{\gamma} = \frac{\sum_{i=1}^{\ell} \sqrt{\lambda_i \sigma_{{\rm c},i}^2}}{\frac{p_{\rm T}}{2} + \sum_{i=1}^{\ell} \sigma_{{\rm c},i}^2}$.

3.2. Estimation of $\sigma_{\rm r}^2$

$\sigma_{\rm r}^2$ depends on $q = n_{\rm SC} - \ell$, $N_{\rm g}$, $\sigma_{\rm I}^2$, and $p_{\rm I}$ [17]. An explicit expression of the evolution of $\sigma_{\rm r}^2$ is very difficult to obtain. Thus, in

this section, we will resort to a phenomenological model (PM) of σ_{r}^2 as a function of these parameters. First experiments have been conducted to characterize the structure of the model. Then the value of the model parameters are estimated via least-square estimation.

Two main channels with $n_{\mathrm{SC}} = 256$ subchannels and $n_{\mathrm{SC}} = 416$ subchannels are considered here. For both channels, Gaussian background noise with $N_{\mathrm{g}} = 2\sigma_{\mathrm{g}}^2 I$ and impulse noise $\sigma_{\mathrm{I}}^2 = 100$ are introduced. The variance of the background noise is adjusted in such a way that the *impulsive to background noise ratio* (INR) in dB, *i.e.*, $10\log_{10}\left(\sigma_{\mathrm{I}}^2/\sigma_{\mathrm{g}}^2\right)$ ranges from 10 dB to 30 dB with a step of 2 dB. The impulse probability p_{I} ranges from 0.5% to 3% with a step of 0.5%. Under these channel conditions, σ_{r}^2 is evaluated, which is obtained as the average of $\|v_{\mathrm{I}} - \widehat{v}_{\mathrm{I}}\|_2^2$, where $\widehat{v}_{\mathrm{I}}$ is obtained from the FBMP algorithm. One evaluates σ_{r}^2 considering different proportions of unused subchannels $r_{\mathrm{d}} = \frac{q}{n_{\mathrm{SC}}}$ ranging from 0.15 to 0.75 with a step of 0.05. Since the FBMP only uses the syndrome (2), which does not depend on the transmitted chunks, all evaluations are performed assuming that all-zero chunks are transmitted.

From the experimental results, one observes that $\log_{10}\left(\sigma_{\mathrm{r}}^2\right)$ can be represented as a function of $(1-r_{\mathrm{d}})^2$, $\mathrm{INR}_{\mathrm{dB}}$ and $\log_{10}(p_{\mathrm{I}})$ and shows an almost linear dependency on each variable when the others are fixed. Therefore one may approximate $\log_{10}\left(\sigma_{\mathrm{r}}^2\right)$ as

$$\log_{10}\left(\sigma_{\mathrm{r}}^2\right) = \mu_0\left(r_{\mathrm{d}}, \mathrm{INR}_{\mathrm{dB}}\right) + \mu_1\left(r_{\mathrm{d}}, \mathrm{INR}_{\mathrm{dB}}\right)\log_{10}\left(p_{\mathrm{I}}\right), \quad (7)$$

where $\mu_i\left(r_{\mathrm{d}}, \mathrm{INR}_{\mathrm{dB}}\right)$, $i = 0, 1$ are considered to have structure as $\mu_i\left(r_{\mathrm{d}}, \mathrm{INR}_{\mathrm{dB}}\right) = \mu_{i,0} + \mu_{i,1}\mathrm{INR}_{\mathrm{dB}} + \mu_{i,2}\left(1-r_{\mathrm{d}}\right)^2 + \mu_{i,3}\left(1-r_{\mathrm{d}}\right)^2\mathrm{INR}_{\mathrm{dB}}$.

Considering all collected data, and using the PM (7), one may easily get a least-square estimate of the value of the parameter vectors $\boldsymbol{\mu}_i = (\mu_{i,0}, \ldots, \mu_{i,3})$, $i = 0, 1$. One gets $\boldsymbol{\mu}_0^{256} = (2.6,\ -0.14,\ -1.71,\ 0.29)$, $\boldsymbol{\mu}_1^{256} = (0.71,\ -0.003,\ -0.92,\ 0.1)$ for the channel with 256 subchannels, $\boldsymbol{\mu}_0^{416} = (2.6, -0.12, -1.79, 0.27)$, $\boldsymbol{\mu}_1^{416} = (0.72,\ 0.007,\ -0.93,\ 0.09)$ for the channel with 416 subchannels. One observes that both sets of parameters have very close values. By using estimated parameter vectors $\boldsymbol{\mu}_0$ and $\boldsymbol{\mu}_1$, in most of the cases, estimated σ_{r}^2s by using model (7) are very close to the values obtained experimentally, since the maximum gap is less than 2.6 . Consequently, the PM (7) provides a good estimate of σ_{r}^2 and can be used in (6) to evaluate the total distortion.

3.3. Optimization of sub-channel provisioning

This section describes the way of optimal provisioning subchannels number q evaluation, which is a function of N_{g}, σ_{I}^2 , p_{I}, p_{T}, n_{SC} and vector of chunk variances $(\lambda_1 \ldots \lambda_{n_{\mathrm{Ck}}})$. Here, one assumes a point-to-point communication.

For a given value of $r_{\mathrm{d}} = \frac{q}{n_{\mathrm{SC}}}$,

1. σ_{r}^2 is deduced from the PM (7),
2. one evaluates the target transmitted chunks number $\ell_{\mathrm{t}} = n_{\mathrm{SC}} - q$,
3. chunk reconstruction MSE $\varepsilon\left(r_{\mathrm{d}}\right)$ is obtained from (6).

At Step 3, the actual transmitted chunk number ℓ may be less than the target number ℓ_{t} due to power constraint [11, 28].

The minimization of $\varepsilon\left(r_{\mathrm{d}}\right)$ may then be performed, *e.g.*, by exhaustive search, or by gradient descent to find

$$\widehat{r}_{\mathrm{d}} = \arg\min_{r_{\mathrm{d}}} \varepsilon\left(r_{\mathrm{d}}\right). \quad (8)$$

The version of the LVC scheme implementing the Optimal Subchannel Provisioning (OSP) with the Impulse noise Correction (IC) is denoted LVC-OSP-IC in what follows.

4. SIMULATION

In this section, three variants of LVC schemes are compared. The first one is baseline LVC with No Impulse noise Correction (LVC-NIC). The number of transmitted chunks is only constrained by the bandwidth and total power constraints. Nevertheless, the effect of the impulse noise is taken into account by an increase of the variance of the background noise from σ_i^2 to $p_{\mathrm{I}}\sigma_{\mathrm{I}}^2 + \sigma_i^2$. The precoding and decoding matrices are adapted accordingly [11, 28]. The second one is LVC-WSP-IC (Section 2). The third one is LVC-OSP-IC (Section 3.3). The simulation parameters are detailed in Section 4.1. Simulation results are described in Section 4.2.

In all cases, metadata have to be transmitted to indicate the indexes and variances of the chunks, the subchannel noise variances of the reference channel, as well as the variance and probability of the impulse noise, *etc*. The amount of side information is of the same order of magnitude as that of plain SoftCast [9] and is neglected in what follows.

4.1. Simulation parameters

Two video sequences are taken from the MPEG test set used for the standardization of HEVC [16], namely BQSquare (Class D) and RaceHorse (Class C). One considers only the luminance component of each video. Consider OFDM subchannels with a bandwidth $f_{\mathrm{SC}} = 24.414$ kHz. Using analog QAM and root-raised-cosine Nyquist filters with $\beta_{\mathrm{r}} = 30\,\%$ roll-off, one obtains a per-subchannel transmission rate $r_{\mathrm{SC}} = \frac{2f_{\mathrm{SC}}}{1+\beta_{\mathrm{r}}}$. The subchannels number n_{SC} for transmission are respectively 256 and 416 for BQSquare and RaceHorses. The GoP size n_{F} is 8 frames. The chunk size $n_{\mathrm{r}} \times n_{\mathrm{c}}$ is 30×32. The frame rare r_{F} is 60 and 30 for BQSquare and RaceHorses respectively. The number of chunks a subchannel can transmit for the duration of a GoP is $\nu_{\mathrm{Ck}} = \frac{n_{\mathrm{F}}}{r_{\mathrm{F}}}\frac{r_{\mathrm{SC}}}{n_{\mathrm{r}}n_{\mathrm{c}}}$. For the typical values of the parameters considered in the simulations, $v_{\mathrm{Ck}} > 1$, *i.e.*, several chunks have to be transmitted on the same subchannel for the duration of a GoP. Therefore at most $n_{\mathrm{TCk}} = \nu_{\mathrm{Ck}}n_{\mathrm{SC}}$ chunks can be transmitted. Moreover the n_{Ck} chunks are ordered by decreasing variance and are partitioned into $n_{\mathrm{gCk}} = \frac{n_{\mathrm{Ck}}}{\nu_{\mathrm{Ck}}}$ groups of ν_{Ck} chunks of similar variance. Consequently, ν_{Ck} precoding (and decoding) matrices have to be designed considering the n_{gCk} chunks of same index in each groups of chunks. In the simulation, we take $\nu_{\mathrm{Ck}} = 3$ for BQSquare and $\nu_{\mathrm{Ck}} = 8$ for RaceHorses. For impulse noise correction, the parameter D used in the FBMP is chosen equal to 5, which represents a compromise between complexity and performance as shown in [17].

4.2. Simulation results

4.2.1. Impact of r_{d} on the efficiency of impulse noise correction

The average PSNR of the first 5 GoPs of BQSquarre and RaceHorses is evaluated for SNRs ranging from 0 dB to 20 dB. This accounts only for the Gaussian noise, while the impulse noise power is considered via the INR. The power constraint p_{t} for one OFDM symbol is set with 2560. The variance and the probability of impulse noise are $\sigma_{\mathrm{I}}^2 = 100$ and $p_{\mathrm{I}} = 0.01$ or $p_{\mathrm{I}} = 0.02$. Figure 2 represents the gains obtained by LVC-WSP-IC compared to LVC-NIC at different SNRs and for different target values of r_{d} taken in $\mathcal{R} = \{0.25, 0.33, 0.41, 0.5, 0.66, 0.75\}$. One observes that the optimal value of r_{d} depends on the value of the channel SNR. At low SNRs, r_{d} should be large, whereas at large SNRs, r_{d} may be reduced. This is mainly due to the fact that at low SNR, the INR is low and impulse noise identification is difficult with few syndrome samples.

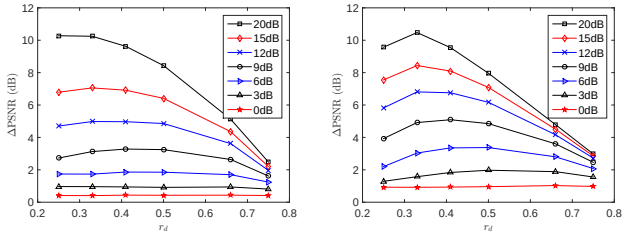

(a) BQSquare when $p_{\mathrm{I}} = 0.01$ (b) RaceHorses when $p_{\mathrm{I}} = 0.02$

Fig. 2: PSNR gain of LVC-WSP-IC compared to LVC-NIC for different r_{d} when $\sigma_{\mathrm{I}}^2 = 100$. (a) BQSquare; (b) RaceHorses.

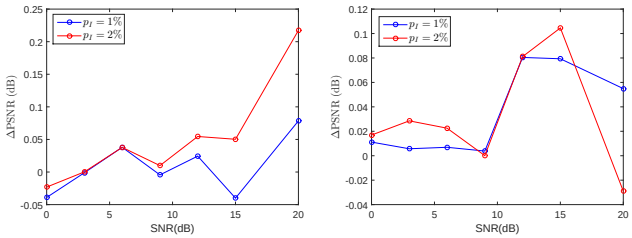

(a) BQSquare (b) RaceHorse

Fig. 3: PSNR differences between LVC-OSP-IC and the best PSNR achieved by LVC-WSP-IC when r_{d} is searched in $\mathcal{R} = \{0.25, 0.33, 0.41, 0.5, 0.66, 0.75\}$

At high SNR, the INR increases, and it becomes easier to identify impulse noise.

4.2.2. *Optimal subchannel provisioning*

Section 3.3 illustrated how to find r_{d} in the case of LVC-OSP-IC, while here we show how to find it in the case of LVC-WSP-IC. Figure 3 represents the PSNR differences between LVC-OSP-IC and LVC-WSP-IC. In most of the cases, LVC-OSP-IC provides better results (positive PSNR difference), since the search for the optimal r_{d} is in a larger set ranging from 0.15 to 0.75 with a step 0.005, and the time to evaluate (6) is negligible. In some cases, LVC-OSP-IC may not perform as well as LVC-WSP-IC due to a mismatch of the PM. Nevertheless, the PNSR loss remains less than 0.05 dB.

Finally, Figure 4 shows reconstructed frames of RaceHorses with LVC-NIC and LVC-OSP-IC when $\sigma_{\mathrm{I}}^2 = 100$, $p_{\mathrm{I}} = 0.01$, SNR $= 15$ dB. A gain of 7.8 dB is observed when the impulse noise mitigation is performed. Reconstructed videos, including one additional test sequence (BasketballDrive) are available at *https://drive.google.com/drive/folders/13LB5nR3nY79bF3CEMUl41HY4Bc_ekhBF*.

4.2.3. *Analysis of the effect of mismatched channel conditions*

In the following experiments, the channel SNR is set equal to 20 dB. One considers several target impulse noise probabilities p_{It} chosen equal to 0%, 0.5%, 1%, or 2% for the LVC-OSP-IC scheme. Then PSNR results for actual impulse noise probabilities p_{I}s ranging from 0% to 4% are shown in Figure 5. In simulation, at receiver side, the parameters of impulse noise correction (FBMP algorithm) and decoding matrix computation (Section 3.1) use the actual channel im-

(a) LVC-NIC: PSNR=30.83dB (b) LVC-OSP-IC: PSNR=38, 64dB.

Fig. 4: First frame of RaceHorses. $\sigma_{\mathrm{I}}^2 = 100$, $p_{\mathrm{I}} = 0.01$ and SNR=15dB. (a) by using LVC-NIC; (b) by using LVC-OSP-IC.

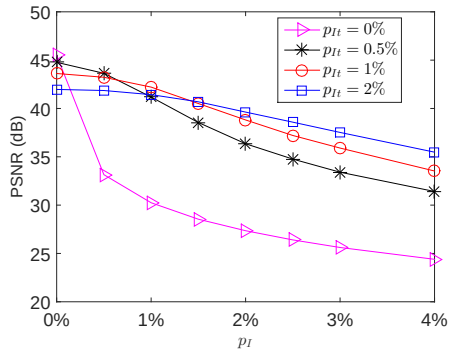

Fig. 5: Effect of the mismatch between the target impulse noise probability p_{It} and the actual impulse noise probability p_{I} when SNR $= 20$ dB (for the RaceHorses video sequence)

pulse noise probability. As expected, the performance is best when p_{I} matches p_{It}. Choosing a large p_{It} improves the robustness to a larger p_{I}, but the price to be paid is a lower PSNR when p_{I} is smaller than p_{It}. It also shows that even if a small $p_{\mathrm{It}} = 0.5\%$ is chosen, in case of mismatch, the PSNR decrease is much smoother than in absence of subchannel provisioning for impulse noise mitigation.

5. CONCLUSION

This paper considers SoftCast-based video transmission scheme affected by impulse noise. FBMP algorithm is adapted for impulse noise mitigation. This requires the provisioning of some subchannels on which no information is transmitted. In this case the nominal PSNR decreases in absence of impulse noise. A trade-off has thus to be found between impulse noise correction efficiency and nominal PSNR reduction.

To address this problem, a PM model proposed to evaluate the variance of the impulse noise residual after mitigation step. This model allows one to estimate optimal number of subchannel to provision for impulse noise correction. The performance of proposed LVC-OSP-IC scheme has been evaluated on two reference video sequences. The performance is significantly better than LVC baseline LVC-NIC.

Future work will be dedicated to the evaluation of the optimal number of subchannels to provision for impulse noise correction in case of LVC under multicast situation.

6. REFERENCES

[1] Tareq Y Al-Naffouri, Ahmed A Quadeer, and Giuseppe Caire. Impulse noise estimation and removal for ofdm systems. *IEEE Transactions on Communications*, 62(3):976–989, 2014.

[2] M. Cagnazzo and M. Kieffer. Shannon-Kotelnikov mappings for SoftCast-based joint source-channel video coding. In *Proc. IEEE ICIP*, pages 1085–1089. IEEE, 2015.

[3] Rafael E Carrillo, Ana B Ramirez, Gonzalo R Arce, Kenneth E Barner, and Brian M Sadler. Robust compressive sensing of sparse signals: a review. *EURASIP Journal on Advances in Signal Processing*, 2016(1):108, 2016.

[4] H. Cui, Z. Song, Z. Yang, C. Luo, R. Xiong, and F. Wu. Cactus: A hybrid digital-analog wireless video communication system. In *Proc. ACM Int. Conf. on Modeling, Analysis & Simulation of Wireless and Mobile Systems*, pages 273–278, 2013.

[5] X. Fan, F. Wu, D. Zhao, and O. C. Au. Distributed wireless visual communication with power distortion optimization. *IEEE Trans. Circuits and Systems for Video Technology*, 23(6):1040–1053, 2013.

[6] X. Fan, R. Xiong, F. Wu, and D. Zhao. Wavecast: Wavelet based wireless video broadcast using lossy transmission. In *Proc. IEEE VCIP*, pages 1–6, San Diego, CA, 2012.

[7] Xiaopeng Fan, Ruiqin Xiong, Debin Zhao, and Feng Wu. Layered soft video broadcast for heterogeneous receivers. *IEEE Trans. Circuits Syst. Video Techn.*, 25(11):1801–1814, 2015.

[8] D. He, C. Lan, C. Luo, E. Chen, F. Wu, and W. Zeng. Progressive pseudo-analog transmission for mobile video streaming. *IEEE Trans. Multimedia*, 19(8):1894–1907, 2017.

[9] S. Jakubczak and D. Katabi. Softcast: Clean-slate scalable wireless video. In *Proc. 48th Annual Allerton Conference on Communication, Control, and Computing*, pages 530–533, 2010.

[10] Cuiling Lan, Chong Luo, Wenjun Zeng, and Feng Wu. A practical hybrid digital-analog scheme for wireless video transmission. *IEEE Transactions on Circuits and Systems for Video Technology*, 28(7):1634–1647, 2018.

[11] K. H. Lee and D. P. Petersen. Optimal linear coding for vector channels. *IEEE Trans. On Communications*, 24(12):1283–1290, 1976.

[12] Jing Lin, Marcel Nassar, and Brian L Evans. Impulsive noise mitigation in powerline communications using sparse bayesian learning. *IEEE Journal on Selected Areas in Communications*, 31(7):1172–1183, 2013.

[13] X. L. Liu, W. Hu, C. Luo, Q. Pu, and F. Wu. Compressive image broadcasting in MIMO systems with receiver antenna heterogeneity. *Signal Processing: Image Communication*, 29(3):361–374, 2014.

[14] X. L. Liu, W. Hu, C. Luo, Q. Pu, F. Wu, and Y. Zhang. Parcast+: Parallel video unicast in MIMO-OFDM WLANs. *IEEE Trans. Multimedia*, 16(7):2038–2051, 2014.

[15] Xiao Lin Liu, Wenjun Hu, Qifan Pu, Feng Wu, and Yongguang Zhang. Parcast: Soft video delivery in mimo-ofdm wlans. In *Proceedings of the 18th annual international conference on Mobile computing and networking*, pages 233–244. ACM, 2012.

[16] J.-R. Ohm, G. J. Sullivan, H. Schwarz, T. K. Tan, and T. Wiegand. Comparison of the coding efficiency of video coding standards–including high efficiency video coding (HEVC). *IEEE Trans. Circuits and Systems for Video Technology*, 22(12):1669–1684, 2012.

[17] Philip Schniter, Lee C Potter, and Justin Ziniel. Fast bayesian matching pursuit. In *Information Theory and Applications Workshop, 2008*, pages 326–333. IEEE, 2008.

[18] Z. Song, R. Xiong, S. Ma, X. Fan, and W. Gao. Layered image/video SoftCast with hybrid digital-analog transmission for robust wireless visual communication. In *Proc. IEEE ICME*, pages 1–6, 2014.

[19] G. J. Sullivan, J.-R. Ohm, W.-J. Han, and T. Wiegand. Overview of the high efficiency video coding (HEVC) standard. *IEEE Trans. Circuits Syst. Video Technol.*, 22(12):1649–1668, 2012.

[20] T. Wiegand, G. J. Sullivan, G. Bjøntegaard, and A. Luthra. Overview of the H.264/AVC video coding standard. IEEE *Trans. on Circuits and Systems for Video Technology*, 13(7):560–576, 2003.

[21] M. Wien, H. Schwarz, and T. Oelbaum. Performance analysis of SVC. *IEEE Trans. Circuits and Systems for Video Technology*, 17(9):1194–1203, 2007.

[22] R. Xiong, F. Wu, X. Fan, C. Luo, S. Ma, and W. Gao. Power-distortion optimization for wireless image/video SoftCast by transform coefficients energy modeling with adaptive chunk division. In *Proc. IEEE VCIP*, pages 1–6, 2013.

[23] R. Xiong, F. Wu, J. Xu, X. Fan, C. Luo, and W. Gao. Analysis of decorrelation transform gain for uncoded wireless image and video communication. *IEEE Trans. Image Processing*, 25(4):1820–1833, 2016.

[24] R. Xiong, J. Zhang, F. Wu, J. Xu, and W. Gao. Power distortion optimization for uncoded linear transformed transmission of images and videos. *IEEE Trans. Image Processing*, 26(1):222–236, 2017.

[25] L. Yu, H. Li, and W. Li. Wireless scalable video coding using a hybrid digital-analog scheme. *IEEE Trans Circuits and Systems for Video Technology*, 24(2):331–345, 2014.

[26] F. Zhang, A. Wang, H. Wang, S. Li, and X. Ma. Channel-aware video SoftCast scheme. In *Proc. IEEE ChinaSIP*, pages 578–581, Chengdu, China, 2015.

[27] Z. Zhang, D. Liu, X. Ma, and X. Wang. Ecast: An enhanced video transmission design for wireless multicast systems over fading channels. *IEEE Systems Journal*, 11(4):2566–2577, 2017.

[28] S. Zheng, M. Antonini, M. Cagnazzo, L. Guerrieri, M. Kieffer, I. Nemoianu, R. Samy, and B. Zhang. SoftCast with per-carrier power-constrained channels. In *Proc. IEEE ICIP*, pages 2122–2126, 2016.

[29] Manfred Zimmermann and Klaus Dostert. Analysis and modeling of impulsive noise in broad-band powerline communications. *IEEE transactions on Electromagnetic compatibility*, 44(1):249–258, 2002.